[Makara Journal of Technology](https://scholarhub.ui.ac.id/mjt)

Volume 19 | Issue 1 Article 1

4-1-2015

Seebeck Coefficient of SOI Layer Induced by Phonon Transport

Faiz Salleh
Research Institute of Electronics, Shizuoka University, 3-5-1 Johoku, Naka-ku, Hamamatsu 432-8011, Japan, faiz@rie.shizuoka.ac.jp

Takuro Oda
Research Institute of Electronics, Shizuoka University, 3-5-1 Johoku, Naka-ku, Hamamatsu 432-8011, Japan

Yuhei Suzuki
Research Institute of Electronics, Shizuoka University, 3-5-1 Johoku, Naka-ku, Hamamatsu 432-8011, Japan

Yoshinari Kamakura
Graduate School of Engineering, Osaka University, 2-1 Yamadaoka, Suita 565-0871, Japan

Hiroya Ikeda
Research Institute of Electronics, Shizuoka University, 3-5-1 Johoku, Naka-ku, Hamamatsu 432-8011, Japan

Recommended Citation

Salleh, Faiz; Oda, Takuro; Suzuki, Yuhei; Kamakura, Yoshinari; and Ikeda, Hiroya (2015) "Seebeck Coefficient of SOI Layer Induced by Phonon Transport," *Makara Journal of Technology*: Vol. 19: Iss. 1, Article 1.
DOI: 10.7454/mst.v19i1.3022
Available at: https://scholarhub.ui.ac.id/mjt/vol19/iss1/1

Makara J. Technol. 19/1 (2015), 1-4
doi: 10.7454/mst.v19i1.3022

Seebeck Coefficient of SOI Layer Induced by Phonon Transport

Faiz Salleh[1*], Takuro Oda[1,2], Yuhei Suzuki[1,3], Yoshinari Kamakura[4], and Hiroya Ikeda[1,2,3]

1. Research Institute of Electronics, Shizuoka University, 3-5-1 Johoku, Naka-ku, Hamamatsu 432-8011, Japan
2. Faculty of Engineering, Shizuoka University, 3-5-1 Johoku, Naka-ku, Hamamatsu 432-8561, Japan
3. Graduate School of Engineering, Shizuoka University, 3-5-1 Johoku, Naka-ku, Hamamatsu 432-8561, Japan
4. Graduate School of Engineering, Osaka University, 2-1 Yamadaoka, Suita 565-0871, Japan

[*]*e-mail: faiz@rie.shizuoka.ac.jp*

Abstract

The Seebeck coefficient of a patterned Si wire on P-doped SOI (Si-on-insulator) layer with a carrier concentration of 10^{18} cm^{-3} was measured near room temperature. The Seebeck coefficient is found to be smaller than that in the SOI layer and to be closer to the calculated Seebeck coefficient including the electronic contribution. The decrease in the Seebeck coefficient of Si wire is likely to occur due to the elimination of the contribution of phonon drag part. From the theoretical calculation of scattering rates by considering the scattering processes in phonon system, it is considered that an increase in phonon-boundary scattering and simultaneously a decrease at the cross section of SOI layer are likely responsible for eliminating the phonon drag effect.

Abstrak

Koefisien Seebeck Lapisan SOI yang Diinduksi oleh Transpor Phonon. Koefisien Seebeck pada kawat Si berpola pada lapisan SOI bersalut-P dengan konsentrasi pembawa sebesar 10^{18} cm^{-3} diukur pada suhu mendekati suhu kamar. Ditemukan bahwa koefisien Seebeck-nya lebih kecil daripada koefisien Seebeck pada lapisan SOI dan lebih dekat pada koefisien Seebeck yang telah diperhitungkan, termasuk kontribusi elektroniknya. Penurunan koefisien Seebeck pada kawat Si mungkin terjadi akibat hilangnya kontribusi bagian tarikan fonon. Dari perhitungan teoretis terhadap rasio-rasio pengacakan yang dilakukan dengan memperhitungkan proses-proses pengacakan di dalam sistem fonon, dapat disimpulkan bahwa kenaikan pengacakan batas-fonon dan penurunan yang terjadi pada bagian simpang dari lapisan SOI secara simultan mungkin menjadi penyebab menghilangnya efek tarikan fonon.

Keywords: seebeck coefficient, phonon drag, Si on insulator

1. Introduction

The low conversion efficiency of converting the thermal energy into electrical energy makes the thermoelectric devices difficult to be applied in daily life. One of the material parameters determining the conversion efficiency of such devices is the Seebeck coefficient S which is defined as a thermo electromotive force (TEMF) generated by a temperature difference. In general, the S of a semiconductor consists of the electronic part S_{elec} and the phonon drag part S_{ph} [1]. S_{elec} is due to the diffusion of carriers (electron in an n-type semiconductor) under a temperature gradient [2], and it is theoretically presumed to increase by nanostructuring [3]. On the other hand, S_{ph} which arises from the electrons dragged by the phonon current due to electron-phonon interactions is considered to be significant at low concentration region [4-7]. In bulk Si material, it is reported that S_{ph} cannot be neglected at room temperature for carrier concentration below 2.2x10^{18} cm^{-3} [4]. Thus, it is necessary to clarify the influence of nanostructure to S_{ph} for near room temperature applications.

Previously, we investigated the S_{ph} values of P-doped ultrathin Si-on-insulator (SOI) layers near room temperature over a carrier concentration range of 10^{17}-10^{19} cm^{-3} [8]. The S_{ph} of SOI layer was found to be significant and depended on the carrier concentration which increases the carrier concentration above ~5x10^{18} cm^{-3} and is likely to originate from the phonon transport rather than the carrier-phonon interaction. Moreover, the

S_{ph} is likely to be independent of the SOI thickness above 9 nm due to the domination of phonon-phonon scattering processes rather than phonon-boundary scattering, in which the sample width is so large that the phonon confinement effect in the thickness direction is insignificant.

Thus, it is necessary to clarify the influence of sample dimension when the dimension of SOI layer is reduced from 2-dimensional shape (thin layer) to 1-dimensional shape (wire) for observing the enhancement in *S*. In the present paper, we investigate the contribution of phonon drag effect to *S* of Si wire which is patterned in a SOI layer in order to clarify the influence of reduction in dimension of SOI layer to S_{ph} near room temperature. In addition, the result is discussed with the theoretical calculation of scattering processes in phonon system.

2. Experiment

The Si wire was fabricated by using conventional SOI wafer consisted of a top Si layer (SOI layer), a buried oxide layer (SiO_2 layer), and a p-type Si substrate. The SOI layer was thinned to a thickness of 82 nm by repeated thermal oxidation and HF etching, as determined by a reflective spectrum film thickness meter. It was doped with P atoms with a carrier concentration of $1x10^{18}$ cm^{-3}, as determined by a four-probe method at room temperature. The array of 10 Si wires was patterned with a width of ~223 nm and a length of 1 mm by SiO_2 mask, electron beam lithography and reactive ion etching. A number of Si wires were patterned instead of a single wire in order to reduce the electrical resistance for making the sample measureable. Si pads with an area of 1.2x0.5 mm^2 were also patterned at both ends of Si wires for TEMF measurement. Al electrodes were deposited and patterned to a size of 0.5x0.5 mm^2 on the Si pads, and another Al electrode was deposited over the entire bottom surface of the p-type Si substrate. Finally, the sample was annealed to form ohmic contacts at the Al/Si interfaces.

Figure 1 shows the schematic diagram of the experimental setup and a typical structure of the fabricated sample used in the present measurement. In this figure, the scanning electron microscope (SEM) image shows the partial array of 10 Si wires. The *S* was measured using the same method as used in our previous study [9,10]. The time evolution of the TEMF was measured simultaneously with the temperature at high- and low-temperature regions in the sample. The temperature was measured in the same temperature location as TEMF probes by thermocouples which align with the probes in normal to give temperature gradient direction. The *S* was evaluated from the gradient of the linear relation between measured TEMF and temperature difference since the *S* is almost constant in

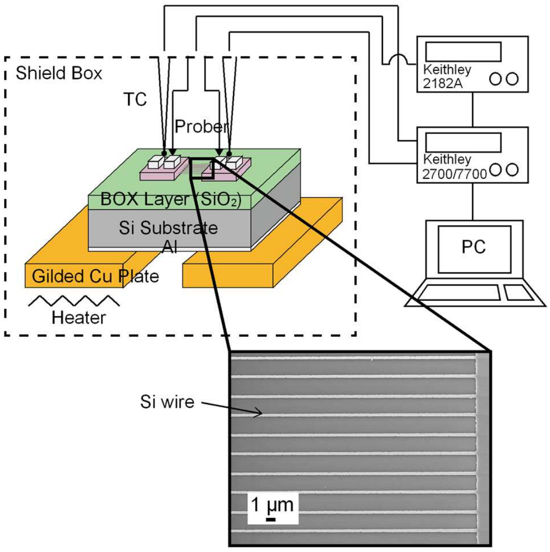

Figure 1. Schematic Diagram of the Apparatus for Measuring the *S* of Si Wire. The Inset shows a SEM Image of Si Wire

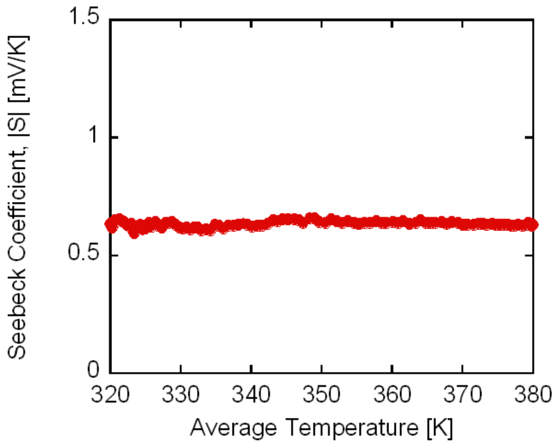

Figure 2. The Measured *S* as a Function of the Average Temperature

the measured temperature range of 320-380 K, as indicated in Fig. 2 where *S* is plotted as a function of the average temperature.

3. Results and Discussion

S evaluated for the Si wire is shown in Fig. 3 as a function of the carrier concentration. In this figure, the previously measured *S* of SOI layers are also shown [9,10]. The numbers adjacent to the filled circles indicate the SOI layer thickness. The broken and dotted lines are the theoretical value of total *S*, S_{total} and S_{elec}, which are calculated by setting the mean-free-path of phonon as a fitting parameter to fit the experimental values of SOI layer at 300 K [8]. The filled square and diamond represent the reported values of Si nanowire, respectively [11,12]. From this figure it is found that the S value of our Si wire is close to S_{elec} and differs from the values of SOI layers. It is also found that the reported values of Si nanowire are close to S_{elec}. Therefore, in the measured Si wire and reported Si nanowires, the contribution of phonon drag becomes much insignificant.

For carrier concentration above 4×10^{19} cm^{-3}, the disappearance in the contribution of phonon drag in Si nanowire is adequately explained by the dependency of S_{ph} on carrier concentration, where S_{ph} is considered to be decreasing along with the increasing of the carrier concentration due to an increase in phonon-impurity scattering [8]. However, the S values of Si wire and Si nanowire with carrier concentration below 1×10^{19} cm^{-3} are still closer to S_{elec} even as the influence of impurities is not significant in low concentration region [8]. Thus, additional factors such as the influence of the sample dimension must be considered since the dimension of the sample is one of the differences between SOI layer and Si wire.

In this study, in order to clarify the influence of sample dimension to S_{ph}, the scattering rate due to phonon-boundary scattering τ_B^{-1}, phonon-phonon umklapp scattering τ_U^{-1} and phonon-phonon normal scattering τ_N^{-1} are calculated by considering only the longitudinal phonon assuming that the phonon energy which contributes to the phonon drag is given by the longitudinal phonon [6]. τ_B^{-1} is calculated by considering the size correction due to the effect of finite sample length and is given by [13]

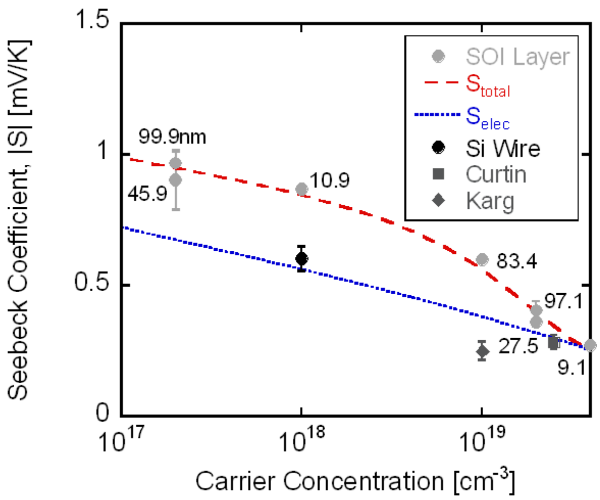

Figure 3. The Absolute *S* of Si Wire as a Function of Carrier Concentration. The *S* of SOI Layers obtained from our Measurement [9,10] and the reported *S* of Si Nanowire are also Shown [11,12]. The Broken and Dotted Lines Represent the S_{total} and S_{elec}, Respectively

$$\tau_B^{-1} = v\left(\frac{1}{1.12(tw)^{0.5}} + \frac{1}{l}\right), \tag{1}$$

where v is the phonon velocity, t and w are the thickness and the width of the sample, respectively, and l is the length of the sample in the direction of heat flow. τ_U^{-1} and τ_N^{-1} are calculated using the expressions [14]

$$\tau_U^{-1} = \frac{\hbar\gamma^2}{Mv^2\theta}\omega^2 T e^{-\frac{\theta}{3T}}, \tag{2}$$

$$\tau_N^{-1} = \frac{k_B^3\gamma^2 V}{M\hbar^2 v^5}\omega^2 T^3, \tag{3}$$

where $\hbar$ is the reduced plank constant, γ is the Grüneisen constant, ω is the angular phonon frequency, M is the average mass of Si, θ is the Debye temperature and T is the absolute temperature.

Figure 4 shows the calculated τ_B^{-1} as a function of width of the Si wire and SOI layers at 300 K. The numbers adjacent to the filled circle indicate the SOI layer thickness. The broken line shows the sum of scattering rate of τ_U^{-1} and τ_N^{-1} ($\tau_P^{-1}=\tau_U^{-1}+\tau_N^{-1}$). For calculating the scattering rates, the reported parameter values in our previous study are used [8], and the lengths of SOI layer and Si wire are 1 cm and 1 mm, respectively. From this figure, it is found that the τ_B^{-1} of Si wire is almost one order higher than the τ_P^{-1}. On the other hand, the τ_B^{-1} of SOI layers even with a thickness as thin as 1 nm are found to be smaller than the τ_P^{-1}. Thus, the S_{ph} of Si wire cannot be meaningfully shown in Fig. 3 if the S_{ph} is also considered to decrease by one order of magnitude. These results qualitatively explain the disappearance of S_{ph} in Si wire and the independency of S_{ph} in SOI layer on SOI thickness. Consequently, the S_{ph} is considered to decrease along with the decreasing of the dimension of SOI layer that is shaped like a Si nanowire due to the domination of phonon-boundary scattering process.

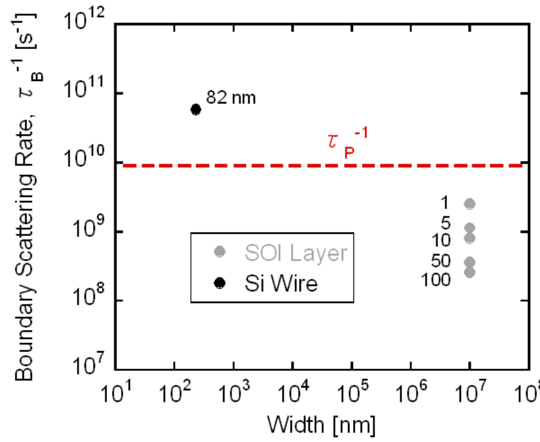

Figure 4. Calculated τ_B^{-1} as a Function of Width. The Broken Line Represents the Calculated τ_P^{-1}

4. Conclusions

We have measured the S of an n-type Si wire with a carrier concentration of 10^{18} cm^{-3}, which was patterned in a SOI layer with a dimension of ~229 nm x 82 nm x 1 mm (width x thickness x length). It is found that the value of S of Si wire is smaller than the values of ultrathin SOI layers, and is closee to the calculated S_{elec}. From the calculated scattering rates due to the phonon-boundary scattering and the phonon-phonon scattering, it is found that the τ_B^{-1} for Si wire is dominant which is in contrast with the case of ultrathin SOI layer where the τ_B^{-1} is still suppressed by τ_P^{-1}. These are in agreement with the facts that the measured S of Si wire is closee to S_{elec} and the measured S of ultrathin SOI layers are not influenced by the SOI thickness. Consequently, it is considered that the reduction in dimension of the SOI layer likely reduces the contribution of phonon drag effect which stood in contrast to the electronic contribution in S.

Acknowledgement

This work was financially supported by a Grant-in-Aid for Challenging Exploratory Research (No. 24651168) from the Japan Society for the Promotion of Science and by Cooperative Research Project of Research Institute of Electronics, Shizuoka University.

References

[1] C. Herring, Phys. Rev. 96 (1954) 1163.
[2] J.P. Jay-Gerin, Phys. Rev. B 12 (1975) 1418.
[3] E.B. Ramayya, L.N. Maurer, A.H. Davoody, I.Knezevic, Phys. Rev. B 86 (2012) 115328.
[4] T.H. Geballe, G.W. Hull, Phys. Rev. 98 (1955) 940.
[5] L. Weber, E. Gmelin, Appl. Phys. A: Mater. Sci. Process. 53 (1991) 136.
[6] E. Behnen, J. Appl. Phys. 67 (1990) 287.
[7] B. Gallagher, J.P. Oxley, T. Galloway, M.J. Smith, P.N. Butcher, J. Phys. Conden. Matter. 2 (1990) 755.
[8] F. Salleh, T. Oda, Y. Suzuki, Y. Kamakura, H. Ikeda, Appl. Phys. Lett. 105 (2014) 102104.
[9] F. Salleh, K. Asai, A. Ishida, H. Ikeda, Appl. Phys. Express. 2 (2009) 071203.
[10] F. Salleh, K. Asai, A. Ishida, H. Ikeda, J. Autom. Mobile Rob. Intell. Syst. 3 (2009) 134.
[11] S. Karg, P. Mensch, B. Gotsmann, H. Schmid, P.D. Kanungo, H. Ghoneim, V. Schmidt, M.T. Björk, V. Troncale, H. Riel, J. Electron. Mater. 42 (2013) 2409.
[12] B.M. Curtin, E.W. Fang, J.E. Bowers, J. Electron. Mater. 41 (2012) 887.
[13] M. Asen-Palmer, K. Bartkowski, E. Gmelin, M. Cardona, A.P. Zhernov, A.V. Inyushkin, E.E. Haller, Phys. Rev. 56/15 (1997) 9431.
[14] D.T. Morelli, J.P. Heremans, G.A. Slack, Phys. Rev. 66/19 (2002) 195304.